A piezomagnetoelastic structure for broadband vibration energy harvesting

A. Erturk,[1,a)] J. Hoffmann,[2] and D. J. Inman[2]

[1]*Department of Engineering Science and Mechanics, Center for Intelligent Material Systems and Structures, Virginia Polytechnic Institute and State University, Blacksburg, Virginia 24061, USA*
[2]*Department of Mechanical Engineering, Center for Intelligent Material Systems and Structures, Virginia Polytechnic Institute and State University, Blacksburg, Virginia 24061, USA*

This letter introduces a piezomagnetoelastic device for substantial enhancement of piezoelectric power generation in vibration energy harvesting. Electromechanical equations describing the nonlinear system are given along with theoretical simulations. Experimental performance of the piezomagnetoelastic generator exhibits qualitative agreement with the theory, yielding large-amplitude periodic oscillations for excitations over a frequency range. Comparisons are presented against the conventional case without magnetic buckling and superiority of the piezomagnetoelastic structure as a broadband electric generator is proven. The piezomagnetoelastic generator results in a 200% increase in the open-circuit voltage amplitude (hence promising an 800% increase in the power amplitude). © *2009 American Institute of Physics.*
[DOI: 10.1063/1.3159815]

Vibration-based energy harvesting has received great attention over the last decade. The basic transduction mechanisms used for vibration-to-electricity conversion are piezoelectric,[1] electromagnetic,[2] electrostatic,[3] and magnetostrictive[4] transductions. Regardless of the transduction mechanism, a primary issue in vibration-based energy harvesting is that the best performance of a generator is usually limited to excitation at its fundamental resonance frequency. If the applied ambient vibration deviates slightly from the resonance condition then the power out is drastically reduced. Hence a major issue in energy harvesting is to enable broadband energy harvesters. Thus researchers have recently focused on the concept of broadband energy harvesting to solve this issue with different approaches.[5,6] This letter introduces a broadband piezoelectric power generator that exhibits large-amplitude periodic oscillations over a frequency range. Although the magnetoelastic structure is discussed here for piezoelectric energy harvesting, it can easily be extended to electromagnetic, electrostatic, and magnetostrictive energy harvesting techniques as well as to their hybrid combinations with similar devices.

The magnetoelastic structure shown in Fig. 1(a) was first investigated by Moon and Holmes[7] as a mechanical structure that exhibits strange attractor motions. The device consists of a ferromagnetic cantilevered beam with two permanent magnets located symmetrically near the free end and it is subjected to harmonic base excitation. The bifurcations of the static problem are described by a butterfly catastrophe with a sixth order magnetoelastic potential. Depending on the magnet spacing, the ferromagnetic beam may have five (with three stable), three (with two stable) or one (stable) equilibrium positions. For the case with three equilibrium positions, the governing lumped-parameter equation of motion has the form of the Duffing equation

$$\ddot{x} + 2\zeta\dot{x} - \tfrac{1}{2}x(1 - x^2) = f \cos \Omega t, \tag{1}$$

where x is the dimensionless tip displacement of the beam in the transverse direction, ζ is the mechanical damping ratio, Ω is the dimensionless excitation frequency, f is the dimensionless excitation force due to base acceleration ($f \propto \Omega^2 X_0$ where X_0 is the dimensionless base displacement amplitude) and an overdot represents differentiation with respect to dimensionless time. The three equilibrium positions obtained from Eq. (1) are $(x,\dot{x})=(0,0)$ (a saddle) and $(x,\dot{x})=(\pm 1,0)$ (two centers). Detailed nonlinear analysis of the magnetoelastic structure shown in Fig. 1(a) can be found in the papers by Moon and Holmes.[7,8]

In order to use this device as a piezoelectric power generator, we attach two piezoceramic layers to the root of the cantilever and obtain a bimorph generator as depicted in Fig. 1(b). The piezoceramic layers are connected to an electrical load (a resistor for simplicity) and the voltage output of the generator across the load due to seismic excitation is the primary interest in energy harvesting. Introducing piezoelectric coupling[1,9,10] into Eq. (1) and applying the Kirchhoff laws to the circuit with a resistive load [Fig. 1(b)] leads to the following electromechanical equations:

$$\ddot{x} + 2\zeta\dot{x} - \tfrac{1}{2}x(1 - x^2) - \chi v = f \cos \Omega t, \tag{2}$$
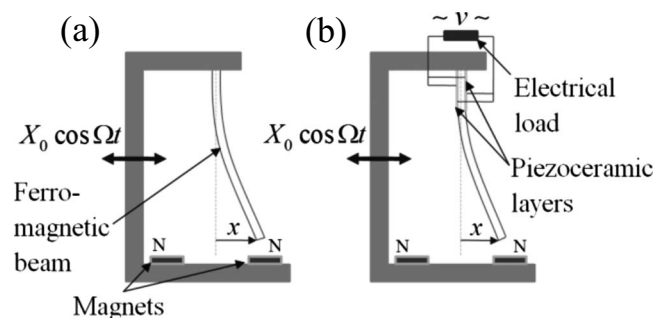

FIG. 1. Schematics of (a) the magnetoelastic structure investigated by Moon and Holmes (Ref. 7) and (b) the piezomagnetoelastic power generator proposed here.

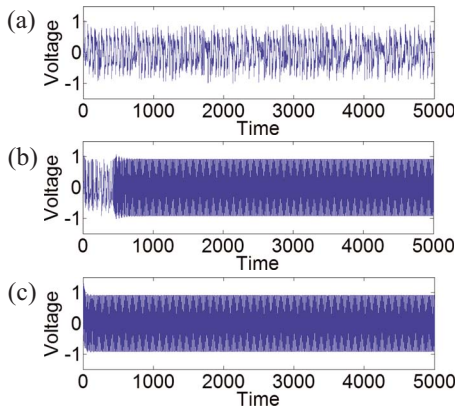a)Author to whom correspondence should be addressed. Electronic mail: erturk@vt.edu.

94, 254102-1

FIG. 2. (Color online) Theoretical voltage histories: (a) Chaotic strange attractor motion ($x(0)=1$, $\dot{x}(0)=0$, $v(0)=0$, and $f=0.083$); (b) Large-amplitude periodic motion due to excitation amplitude ($x(0)=1$, $\dot{x}(0)=0$, $v(0)=0$, and $f=0.115$); (c) Large-amplitude periodic motion due to initial conditions ($x(0)=1$, $\dot{x}(0)=1$, $v(0)=0$, and $f=0.083$).

$$\dot{v} + \lambda v + \kappa \dot{x} = 0, \tag{3}$$

where v is the dimensionless voltage across the load resistance, χ is the dimensionless piezoelectric coupling term in the mechanical equation, κ is the dimensionless piezoelectric coupling term in the electrical circuit equation, and λ is the reciprocal of the dimensionless time constant ($\lambda \propto 1/R_l C_p$ where R_l is the load resistance and C_p is the equivalent capacitance of the piezoceramic layers).[1,9,10]

Time domain simulations of the voltage response for different excitation amplitudes and initial conditions are shown in Fig. 2 (for $\Omega = 0.8$, $\zeta = 0.01$, $\chi = 0.05$, $\kappa = 0.5$, and $\lambda = 0.05$). The first case given by Fig. 2(a) starts with an initial deflection at one of the stable equilibrium positions [$x(0)=1$ with zero initial velocity and voltage: $\dot{x}(0)=v(0)=0$] and results in a chaotic voltage response on a strange attractor [the Poincaré map of this strange attractor motion is later given by Fig. 5(a)]. If the excitation amplitude is increased by keeping the same initial conditions as in Fig. 2(b), the transient chaotic behavior is followed by a large-amplitude periodic motion (limit cycle oscillation) with increased voltage response. More importantly, Fig. 2(c) shows that this type of large-amplitude voltage response can be obtained with the original excitation amplitude [of Fig. 2(a)] with different initial conditions [simply by imposing an initial velocity condition so that $x(0)=\dot{x}(0)=1$, $v(0)=0$].

The piezomagnetoelastic generator and the setup used in the experiments are shown in Fig. 3. Harmonic base excitation is provided by a seismic shaker, acceleration at the base of the cantilever is measured by a small accelerometer, and the velocity response of the cantilever is recorded by a laser vibrometer. The ferromagnetic beam (made of tempered blue steel) is 145-mm-long (overhang length), 26-mm-wide, and
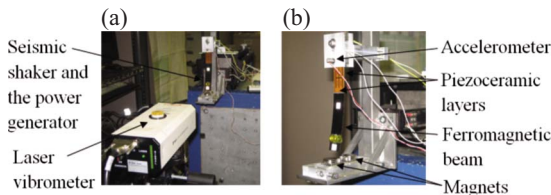

FIG. 3. (Color online) (a) A view of the experimental setup and (b) the piezomagnetoelastic power generator.
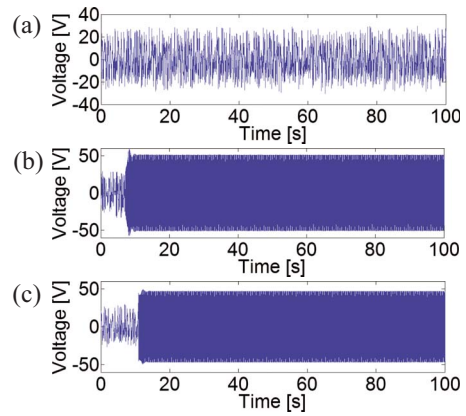

FIG. 4. (Color online) Experimental voltage histories: (a) Chaotic strange attractor motion (excitation: $0.5g$ at 8 Hz); (b) Large-amplitude periodic motion due to the excitation amplitude (excitation: $0.8g$ at 8 Hz); (c) Large-amplitude periodic motion due to a disturbance at $t=11$ s (excitation: $0.5g$ at 8 Hz).

0.26-mm-thick. A lumped mass of 14 g is attached close to the tip for improved dynamic flexibility. Two PZT-5A piezoceramic layers (QP16N, Midé Corporation) are attached onto both faces of the beam at the root using a high shear strength epoxy and they are connected in parallel. The spacing between the symmetrically located circular rare earth magnets is 50 mm (center to center) and this distance is selected to realize the three equilibrium case described by Eqs. (2) and (3). The tip deflection of the magnetically buckled beam in the static case to either side is approximately 15 mm relative to the unstable equilibrium position ($x=0$). The postbuckled fundamental resonance frequency of the beam is 10.6 Hz whereas the fundamental resonance frequency of the unbuckled beam (when the magnets are removed) is 7.4 Hz (both under the open-circuit conditions of piezoceramics, i.e., at constant electric displacement).

For a harmonic excitation amplitude of $0.5g$ (where g is the gravitational acceleration: $g=9.81$ m/s^2) at 8 Hz with an initial deflection at one of the stable equilibrium positions (15 mm to the shaker side), zero initial velocity and voltage, the chaotic open-circuit voltage response shown in Fig. 4(a) is obtained [the Poincaré map of the strange attractor motion is later given by Fig. 5(b)]. If the excitation amplitude is increased to $0.8g$ (at the same frequency), the structure goes
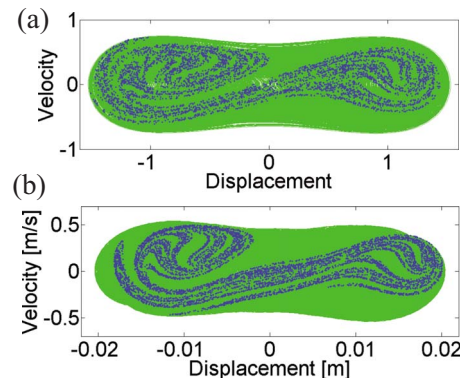

FIG. 5. (Color online) Example phase portraits and Poincaré maps of the chaotic motions exhibiting strange attractors: (a) Theoretical ($x(0)=1$, $\dot{x}(0)=0$, $v(0)=0$, $\Omega=0.8$, $\zeta=0.01$, $f=0.083$, $\chi=0.05$, $\kappa=0.5$, and $\lambda=0.05$) and (b) Experimental (initial tip displacement: 15 mm, zero initial tip velocity, zero initial voltage, excitation: $0.5g$ at 8 Hz).

from transient chaos to a large-amplitude periodic (limit cycle) motion with a strong improvement in the voltage response as shown in Fig. 4(b). A similar improvement is obtained in Fig. 4(c) where the excitation amplitude is kept as the original one (0.5*g*) and a disturbance (hand impulse) is applied at *t*=11 s (as a simple alternative to creating a velocity initial condition). Such a disturbance can be realized in practice by applying an impulse type voltage input through one of the piezoceramic layers for an instant. The experimental evidence given with Fig. 4 is in agreement with the theoretical discussion given with Fig. 2. The Poincaré maps of the theoretical [Fig. 2(a)] and the experimental [Fig. 4(a)] strange attractor motions are in very good qualitative agreement (Fig. 5). Noticing the large-amplitude voltage response obtained at an *off-resonance* frequency in Figs. 4(b) and 4(c), the broadband performance of the device is investigated next.

For a harmonic base excitation amplitude of 0.5*g* [yielding a root-mean-square (rms) acceleration of 0.35*g*], experiments are conducted at 4.5, 5, 5.5, 6, 6.5, 7, 7.5, and 8 Hz. At each frequency, a large-amplitude periodic response is obtained the same way as in Fig. 4(c) with a disturbance around *t*=11 s. Then the magnets are removed for comparison of the device performance with that of the conventional piezoelastic configuration and the base excitation tests are repeated for the same frequencies with approximately the same input acceleration. The open-circuit rms voltage outputs of the piezomagnetoelastic and piezoelastic configurations at each frequency are obtained considering the steady-state response in the 80–100 s time interval. The rms values of the input base acceleration are also extracted for the same time interval. Figure 6(a) shows that the excitation amplitudes of both configurations are very similar (with an average rms value of 0.35*g*). The broadband performance of the piezomagnetoelastic generator is shown in Fig. 6(b). The resonant piezoelastic device gives larger voltage output only when the excitation frequency is at or very close to its resonance frequency (7.4 Hz) whereas the voltage output of the piezomagnetoelastic device can be three times that of the piezoelastic device at several other frequencies below its postbuckled resonance frequency (10.6 Hz). It should be noted that power
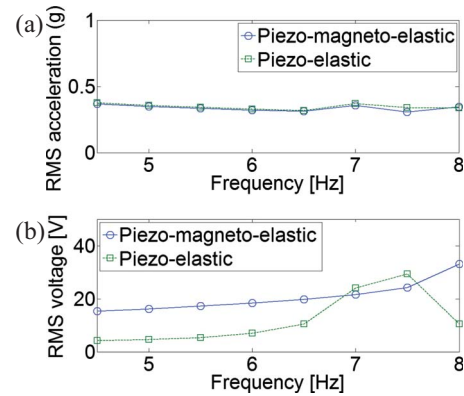

FIG. 6. (Color online) (a) rms acceleration input at different frequencies (average value: 0.35*g*); (b) Open-circuit rms voltage output over a frequency range showing the broadband advantage of the piezomagnetoelastic generator.

output is proportional to the square of the voltage. Hence an order of magnitude larger power output over a frequency range can be expected with this device. The idea proposed here can also be employed in electromagnetic, electrostatic, and magnetostrictive energy harvesting applications with similar magnetoelastic devices.

[1] A. Erturk and D. J. Inman, Smart Mater. Struct. **18**, 025009 (2009).
[2] S. P. Beeby, R. N. Torah, M. J. Tudor, P. Glynne-Jones, T. O'Donnell, C. R. Saha, and S. Roy, J. Micromech. Microeng. **17**, 1257 (2007).
[3] P. D. Mitcheson, P. Miao, B. H. Stark, E. M. Yeatman, A. S. Holmes, and T. C. Green, Sens. Actuators, A **115**, 523 (2004).
[4] L. Wang and F. G. Yuan, Smart Mater. Struct. **17**, 045009 (2008).
[5] M. S. M. Soliman, E. M. Abdel-Rahman, E. F. El-Saadany, and R. R. Mansour, J. Micromech. Microeng. **18**, 115021 (2008).
[6] B. Marinkovic and H. Koser, Appl. Phys. Lett. **94**, 103505 (2009).
[7] F. C. Moon and P. J. Holmes, J. Sound Vib. **65**, 275 (1979).
[8] P. Holmes, Philos. Trans. R. Soc. London, Ser. A **292**, 419 (1979).
[9] A. Erturk and D. J. Inman, ASME J. Vibr. Acoust. **130**, 041002 (2008).
[10] A. Erturk, O. Bilgen, and D. J. Inman, Appl. Phys. Lett. **93**, 224102 (2008).